CONSTRAINTS OF MELTING, SEA-LEVEL AND THE PALEOCLIMATE FROM GRACE

NNG04GF09G

Annual Report No. 1

For the Period 14 March 2004 through 13 March 2005

Principal Investigator

Dr. James L. Davis

March 2005

Prepared for

National Aeronautics and Space Administration
Goddard Space Flight Center, Greenbelt, MD

Smithsonian Institution
Astrophysical Observatory
Cambridge, Massachusetts 02138

The Smithsonian Astrophysical Observatory is a member of the Harvard-Smithsonian Center for Astrophysics

Annual Report for

NASA Grant NNG04GF09G

Constraints on Melting, Sea Level and the Paleoclimate from GRACE

For the period 14 March 2004 through 13 March 2005

Main Results

To gauge the accuracy of the GRACE data, we have undertaken a study to compare deformations predicted by GRACE inferences of seasonal water loading to crustal position variations determined from GRACE data. Two manuscripts that resulted from this study are attached. We found a very high correlation between the GRACE and GPS determinations for South America [*Davis et al.*, 2004]. We also developed a statistical approach for choosing which Stokes coefficients to include. This approach proves to be somewhat more accurate than the traditional Gaussian filter [*Davis et al.*, 2005].

Attachments

Davis, J. L., P. Elósegui, J. X. Mitrovica, and M. E. Tamisiea, Climate-driven deformation of the solid earth from GRACE and GPS, *Geophys. Res. Lett.*, *31*, L24605, doi:10.1029/2004GL021435, 2004.

Davis, J. L., P. Elósegui, M. E. Tamisiea, and J. X. Mitrovica, Regional deformation studies with GRACE and GPS, submitted to *Adv. Geosci.*, 2005.

Regional Deformation Studies with GRACE and GPS

J. L. Davis[1], P. Elósegui[1,*], M. Tamisiea[1], and J. X. Mitrovica[2]

[1]Harvard-Smithsonian Center for Astrophysics, Cambridge, Massachusetts, USA
[2]Department of Physics, University of Toronto, Toronto, Ontario, Canada
[*]Also at Institut Estudis Espacials Catalunya/CSIC, Barcelona, Spain

Manuscript submitted to

ADVANCES IN GEOSCIENCES

Manuscript version from 30 November 2004

Offset requests to:
J. L. Davis
Harvard-Smithsonian Center for Astrophysics
60 Garden St., MS 42
Cambridge, MA 02138 USA

Send proofs to:
J. L. Davis
Harvard-Smithsonian Center for Astrophysics
60 Garden St., MS 42
Cambridge, MA 02138 USA

Abstract

GRACE data indicate large seasonal variations in gravity that have been shown to be to be related to climate-driven fluxes of surface water. Seasonal redistribution of surface mass deforms the Earth, and our previous study using GRACE data demonstrate that annual radial deformations of ± 13 mm in the region of Amazon River Basin were observed by both GRACE and ten GPS sites in the region. For the GRACE determinations, we estimate in a least-squares solution for each Stokes coefficient parameters that represent the amplitudes of the annual variation. We then filter these parameters based on a statistical test that uses the scatter of the postfit residuals. We demonstrate by comparison to the GPS amplitudes that this method is more accurate, for this region, than Gaussian smoothing. Our model for the temporal behavior of the gravity coefficients includes a rate term, and although the time series are noisy, the glacial isostatic adjustment signal over Hudson's Bay can be observed.

Correspondence to: J. L. Davis (jdavis@cfa.harvard.edu)

1 Introduction

The GRACE mission is providing a unique opportunity for studying the Earth's global gravity variations. At seasonal timescales, the most significant mass motions are associated with climate-driven transport of water on the surface of the Earth. This redistribution of water on the surface of the Earth will act as a change in the surface load and will deform the Earth.

GRACE is therefore a potential tool for inferring loading-induced deformation of the solid Earth over timescales greater than about one month, the approximate time required to produce a global gravity field. This temporal coverage may be compared to surveying with the Global Positioning System (GPS) in "continuous" mode, in which estimates of site position may be made by combining data acquired every 24 hours or less. GRACE recovers the gravity variations, and the surface mass redistributions derived from them, with global coverage of high spatial resolution (typically up to degree $\ell = 120$). GPS observations are acquired from a generally sparse (but in some places very dense) network that is highly heterogeneous, especially in regard to the southern hemisphere and the oceans.

GRACE and GPS are thus complementary approaches for studying loading-induced deformation of the solid Earth. GRACE has no information at $\ell = 1$, for example, whereas GPS has been used for several years to detect the deformation at this degree (Blewitt et al., 2001). Recovering deformation at higher degrees poses difficulty for GPS, however (Blewitt et al., 2003), whereas for GRACE it is natural.

In Davis et al. (2004) we compared estimates from GRACE and GPS of annual amplitudes of radial deformation for South America, and demonstrated that there is a significant correlation. In that work, we briefly discussed a statistical approach for filtering the estimated annual amplitudes. Below we extend our calculations for the existing GRACE data set, and investigate the accuracy of the statistical filtering approach by comparing the results to those obtained using a more standard Gaussian smoothing approach.

2 Calculation of radial deformation

A GRACE Level-2 data set (Bettadpur, 2003) consists of Stokes coefficients representing an expansion in spherical harmonics of the Earth's gravity potential. Each data set results from the reduction of approximately one month of GRACE observations consisting primarily of the range between the co-orbiting satellites. Corrections are applied for oceanic and atmospheric mass motions on timescales shorter than one month (Flechtner, 2003). Changes in the Stokes coefficients can be used to calculate changes in the geoid $\Delta N(\phi, \lambda)$ at a point on the surface of the Earth with latitude ϕ and longitude λ using

$$\Delta N(\phi, \lambda) = a \sum_{\ell=2}^{\infty} \sum_{m=0}^{\ell} P_{\ell m}(\sin \phi) [\Delta C_{\ell m} \cos m\lambda$$

$$+ \Delta S_{\ell m} \sin m\lambda \Big] \tag{1}$$

where a is the radius of the Earth, $P_{\ell m}(\sin\phi)$ are the fully normalized associated Legendre functions (Bettadpur, 2003), $\Delta C_{\ell m}$ and $\Delta S_{\ell m}$ are changes in the dimensionless Stokes coefficients at degree ℓ and order m. (The summation begins at $\ell = 2$ because, as mentioned above, GRACE has no information at $\ell = 1$.) Wahr et al. (1998) showed that a change is surface mass density $\Delta\sigma(\phi, \lambda)$ can be calculated from a change in the Stokes coefficients using

$$\Delta\sigma(\phi,\lambda) = \frac{a\rho_e}{3} \sum_{\ell=2}^{\infty} \sum_{m=0}^{\ell} \left(\frac{2\ell+1}{1+k_\ell}\right) P_{\ell m}(\sin\phi) \times \left[\Delta C_{\ell m} \cos m\lambda + \Delta S_{\ell m} \sin m\lambda\right] \tag{2}$$

where ρ_e is the average density of the Earth and k_ℓ is the elastic gravity load-Love number for degree ℓ (Farrell, 1972).

If we assume that temporal changes the observed GRACE coefficients represent changes in the surface mass, then the gravitational load of this surface mass will deform the surface of the Earth. The elastic Green's function $G(\gamma)$ for radial displacement for a point an angular distance γ from the point load (Farrell, 1972) is

$$G(\gamma) = \frac{a}{m_e} \sum_{\ell=0}^{\infty} h_\ell P_\ell(\cos\gamma) \tag{3}$$

where h_ℓ is the elastic deformation load-Love number for degree ℓ and m_e is the mass of the Earth. The radial deformation $\Delta r(\phi, \lambda)$ for an arbitrary surface load $\Delta\sigma(\phi, \lambda)$ is

$$\Delta r(\phi,\lambda) = a^2 \iint d\Omega' \; \Delta\sigma(\phi',\lambda') \; G(\gamma) \tag{4}$$

with the integration performed over the entire surface of the Earth, and where $d\Omega' = d\phi' d\lambda' \cos\phi'$ and $\cos\gamma = \sin\phi\sin\phi' + \cos\phi\cos\phi'\cos(\lambda - \lambda')$. Using Eqs. (2) and (3) in Eq. (4), and using the Addition Theorem to express $\cos\gamma$, yields

$$\Delta r(\phi,\lambda) = a \sum_{\ell=2}^{\infty} \sum_{m=0}^{\ell} \left(\frac{h_\ell}{1+k_\ell}\right) P_{\ell m}(\sin\phi) \times \left[\Delta C_{\ell m} \cos m\lambda + \Delta S_{\ell m} \sin m\lambda\right] \tag{5}$$

3 Temporal variation of gravity

Visual inspection of time series of observed Stokes coefficients leads us to conclude that there is a strong annual component to the temporal variation of gravity. With just slightly over a 2-year timespan, some apparently "secular" (or at least longer-term) variation is also visible in some of the time series. So that this longer-term variation does not systematically bias estimates of the annual variation, we include a rate term in our analysis. Thus, our models for the Stokes coefficients is

$$C_{\ell m}(t) = C^{\circ}_{\ell m} + \dot{C}_{\ell m}\Delta t + C^{a,i}_{\ell m} \cos 2\pi f \Delta t + C^{a,o}_{\ell m} \sin 2\pi f \Delta t \tag{6}$$

where $C^{\circ}_{\ell m}$ is a constant value, $\dot{C}_{\ell m}$ is a rate term, $C^{a,i}_{\ell m}$ and $C^{a,o}_{\ell m}$ are annual amplitudes, and $\Delta t = t - t_{\circ}$. (Superscript "i" stands for "in-phase" and "o" for "out-of-phase.") The frequency f is one cycle per year, and we used $t_{\circ} = 2003.0$.

Fig. 1 shows example time series for two Stokes coefficients, $C_{8,1}$ and $C_{33,0}$. The error bars used are the formal errors from the Level-2 data files. The time series for $C_{8,1}$ has a pronounced sinusoidal term as well as a visible secular variation, whereas the time series for $C_{33,0}$ has neither.

The fitting procedure enables us to evaluate the GRACE data noise. Following Wahr et al. (2004), we define the "realistic" errors $\delta C_{\ell m}$ and $\delta S_{\ell m}$ to be the weighted root-mean-square (wrms) residual to Eq. (6) using the best-fit (i.e., least-squares) parameter estimates for each degree and order. The error degree amplitude δN_{ℓ} is then

$$\delta N_{\ell} = a \sqrt{\sum_{m=0}^{\ell} (\delta C^2_{\ell m} + \delta S^2_{\ell m})} \tag{7}$$

The observed error degree amplitude is shown in the top frame of Fig. 2. The baseline GRACE values require a scaling of ~47 to achieve equality with the observed values. Wahr et al. (2004) found a value of 40 for the scaling, but they included degrees between 70 and 120, for which a smaller scaling is required (as can be seen from their figure).

Using the scaling factor of 47, we can calculate realistic error degree amplitudes for the rate and annual-amplitude parameters of Eq. (6) and compare these to the degree amplitudes calculated using the parameter values. These are shown in the center (annual amplitude) and bottom (rate) frames of Fig. 2. For the seasonal terms, the estimated signal exceeds the error only for $\ell < 15$ or so, in agreement with (Wahr et al., 2004). The rate signal exceeds the error only modestly for all degrees except for $\ell = 2$; the $C_{2,0}$ term shows a large signal of currently unknown origin.

4 Filtering the annual signal

A common way of filtering the coefficients to enhance the contribution of a signal at low degrees and decreasing the contribution of noise at high degrees is to use an azimuthally symmetric Gaussian averaging function of Jekeli (1981). In the spherical harmonic domain, this function depends on degree only. However, we observe that the annual signal is not necessarily significant at all orders, even if the degree amplitude is significantly greater than the error. As an alternative, we explore a statistical approach.

When the errors are not well known, we base the significance of the annual terms on a hypothesis test for the significance of the improvement of the fit when the annual terms are included compared to when they are fixed to zero. If we have N epochs, then the least-squares solution has $N - 4$ degrees of freedom when the model Eq. (6) is used. If the annual terms are fixed to zero, the solution has $N - 2$ degrees of freedom. If χ^2_1 is the postfit χ^2 statistic with $N - 2$ degrees of freedom and

χ_2^2 with $N-4$ degrees of freedom, we form the statistic

$$\Phi = \frac{N-4}{2}\left(\frac{\chi_1^2 - \chi_2^2}{\chi_2^2}\right) \tag{8}$$

Under the hypothesis that the "true" model contains no annual terms, the numerator of the term in parentheses of Eq. (8) is the difference between χ^2 statistics calculated for $N-2$ and $N-4$ degrees of freedom, and is therefore has a χ^2 distribution with 2 degrees of freedom. The denominator of the term in parentheses has a χ^2 distribution with $N-4$ degrees of freedom. Under the hypothesis, then, the Φ has an F-distribution with $(2, N-4)$ degrees of freedom and an expectation of unity.

A large difference between the χ^2 statistic with and without the annual terms estimated would indicate that these terms "absorb" variation relative to the residual variation. This situation would lead to a large Φ value compared to the expectation of unity under the hypothesis. If the annual terms absorb little or no variation, a small Φ value would result. We can reject the hypothesis of no annual variations if the Φ statistic is greater than some confidence limit for the F-statistic. We therefore choose only the set of (ℓ, m) pairs for which we reject the null hypothesis. We will call this set Ω, so that we use only $\ell, m \in \Omega$.

A problem presents itself in that we perform the fit and the F-test separately for the C and S Stokes coefficients. We have investigated two ways of handling this issue. In the first approach, we define the inclusion set Ω_C for the C coefficients and Ω_S for the S coefficients. Another approach would be to define $\ell, m \in \Omega$ if the F-test for either the C or S coefficient indicated significance, yielding

$$\begin{aligned}\Delta r^a(\phi,\lambda) = a \sum_{\ell,m\in\Omega}\left(\frac{h_\ell}{1+k_\ell}\right) P_{\ell m}(\sin\phi) \\ \times \left[\Delta C^a_{\ell m}\cos m\lambda + \Delta S^a_{\ell m}\sin m\lambda\right]\end{aligned} \tag{9}$$

Here the superscript a indicates either in-phase or out-of-phase annual amplitudes, calculated from our fit to Eq. (6). Because it does not make a significant difference for this data set, we will use this simpler approach for the following calculations.

5 Observed annual deformations

Our data consisted of 22 Level-2 GRACE data sets acquired between 2002.33 and 2004.54. Most of these data files contained Stokes coefficients with $\ell \leq 120$, although several had only $\ell \leq 70$. We therefore limited our analysis to $\ell \leq 70$. Using the time series for each Stokes coefficient, we used least-squares to estimate the parameters of Eq. (6). We also performed the solution with the annual terms constrained to zero, so that the Φ statistic of Eq. (8) could be calculated. We then formed the set Ω of degree/order pairs that exceeded the 99.99% level of confidence for an F-distribution with (2,18) degrees of freedom. The Φ statistic for 94 degree/order pairs exceeded this level of confidence.

Fig. 3 shows the observed global in-phase and out-of-phase annual radial deformation amplitudes. The largest deformation amplitudes are in areas where previous works (Tapley et al., 2004; Wahr et al., 2004) indicate the largest amplitudes of inferred annual surface water amplitudes. The deformation signal is largest in the Amazon Basin, sub-Saharan Africa, and southeast Asia. In the latter two regions, the amplitude of the deformation is ~6 mm. In the Amazon basin, the deformation signal is twice as large.

The deformation field of Fig. 3 shows a number of smaller amplitude features, and the F-test filtering technique we applied does not yield for the largest features the round "bull's eye" shape that Gaussian smoothing yields (Tapley et al., 2004; Wahr et al., 2004). In Fig 4 we show in larger scale the observed global deformations for South America calculated in three ways: the F-test filter describe in Sec. 4 (top) and Gaussian-smoothing of the complete set of coefficients with radii of 1000 km (middle) and 300 km (bottom). (We will refer to the deformation amplitudes determined using the F-test procedure as "filtered" and those produced with Gaussian smoothing as "smoothed.") The Gaussian smoothing with a radius of 1000 km yields much "rounder" deformation patterns. The filtered deformations yields a deformation pattern that is highly elongated in the east-west direction. Because of this, Gaussian smoothing with a radius of 1000 km also yields smaller total deformation amplitudes, as the smoothing averages in values to the north and south that fall off to zero more rapidly. Gaussian smoothing with a radius of 300 km preserves the amplitude, but a great deal of "streaking" associated with GRACE errors is evident. The filtered reconstruction also shows 1–2 mm in-phase amplitudes throughout the southern portion of South America, whereas these amplitudes fall off in distance from the Amazon for the 1000-km-smoothed reconstruction.

Davis et al. (2004) compared annual amplitudes of radial deformation from Global Positioning System (GPS) sites in South America to those determined from GRACE, and found a very high correlation. Here, we repeat those calculations for the extended GRACE data set and also reconstruct the deformations using Gaussian smoothing. We then use the GPS-GRACE comparison to address the question of which of the three reconstructions (F-test filtering, Gaussian smoothing with 300 km radius, or Gaussian smoothing with 1000 km radius) yields more accurate amplitudes.

To compare these two data types, we must first correct for the absence of the $\ell = 1$ term in the GRACE data. This correction procedure is described by Davis et al. (2004). Briefly, we use the GPS-GRACE residuals to estimate three parameters representing the cartesian components of the annual amplitude of the geocenter variations, which express themselves as the $\ell = 1$ term. We then use these parameter estimates to "correct" the GRACE amplitudes for the $\ell = 1$ term. The determination of the $\ell = 1$ corrections were done independently for the filtered and smoothed GRACE estimates.

The GRACE-GPS comparisons are shown in Fig. 5. Each comparison displays a reasonably high correlation. The weighted root-mean-square GPS-GRACE difference is 1.5 mm for the filtered values, 1.8 mm for the 1000-km-smoothed, and 1.6 mm for the 300-km-smoothed. One large contribution to the better performance of the smaller smoothing radius compared to the larger smoothing

radius is that the larger amplitude seen in the GPS data is captured better. As discussed above, the larger smoothing radius averages out the larger amplitudes. This effect can be seen in Fig. 6, which shows the wrms GRACE-GPS fit for a range of soothing radii. Starting at 1000 km, decreasing the smoothing radius improves the fit (decreases the wrms) until, for radii less than ~300 km, the errors in the high-degree terms begin to dominate the comparison. However, visual inspection of Fig. 4 indicates that a large amount of noise is apparent at a smoothing radius of 300 km. Thus, the fit of such a solution would depend critically on the geographical sampling represented by the GPS sites.

The filter approach recovered the geographic pattern of annual deformation slightly better than the smoothing approach. It enabled the inclusion of higher degree terms that better define the shape of the deformation without introducing the "streaks." However, a number of other larger-scale features appear (see Fig. 3) that we are unable to determine, without further investigation, whether they are real.

6 Observed rates

The time series of $C_{8,1}$ in Fig. 1 showed a definite linear trend. We might therefore ask whether any significant rates can be observed. Our model Eq. (6) contained a term representing a rate, and so it is a matter of reconstructing a rate field using these estimated parameters. The F-test method does not work reliably on this parameter, probably because there is only one degree of freedom (i.e., one parameter is being tested), and the rate estimate is extremely sensitive to outliers, especially near the beginning and end of such a short time series. We therefore choose to reconstruct the field using Gaussian smoothing, and we look at the geoid rate, since we expect to encounter secular variation of gravity not associated with elastic loading but also with glacial isostatic adjustment (GIA). However, we expect at this stage to see a number of other signals that are not truly secular but that are absorbed by a rate parameter linear over the two-year timespan of GRACE data.

Although the observed geoid rates (Fig. 7) appear noisy, the observed values are well within reasonable bounds. In particular, the rate of change of the geoid over Hudson's Bay in North America is ~1.1 mm yr^{-1}, consistent with the range of expectations (Wahr and Davis, 2002). The largest negative signal -1.6 mm yr^{-1} is over the Gulf of Alaska, where glacier melting is contributing ~0.3 mm yr^{-1} of globally averaged sea-level change (Tamisiea et al., 2004). A longer time series will be required to determine the reliability of these and other features evident in Fig. 7.

7 Conclusions

The F-test "filter" performs better than Gaussian smoothing for the annual amplitudes in South America. It admits some high spatial frequencies into the solution and removes others whose coefficients do not exhibit significant annual variation. As a result, for example, the east-west elongation of the deformation is observed that cannot be observed by smoothing. Preliminary studies indicate

that this approach works well on a global network for which the amplitudes are in general much less, although there are regional variations in correlation (Elósegui et al., 2004).

Although the rates estimates, which result from the same solutions as the annual amplitudes, are noisy, at least one known signal can be observed, GIA in Hudson's Bay. Of course, the goal of GRACE is to measure unknown signals. It is difficult to know at this early stage, however, which of the signals are truly secular.

Acknowledgements. This research was supported by NASA grants NNG04GF09G, NNG04GL69G, and NAG5-13748, and by both the Natural Sciences and Engineering Research Council of Canada and the Miller Institute for Basic Sciences (JXM). Some figures were generated using Generic Mapping Tools version 3 (Wessel and Smith, 1995).

References

Bettadpur, S., *Level-2 Gravity-Field Product User Handbook*, CSR-GR-03-01, Rev. 1, 2003.

Blewitt, G., D. Lavaleé, P. Clarke, and K. Nurutdinov, A new global mode of Earth deformation: Seasonal cycle detected, *Science*, *294*, 2342–2345, 2001.

Blewitt, G., and P. Clarke, Inversion of Earths changing shape to weigh sea level in static equilibrium with surface mass redistribution, *J. Geophys. Res.*, *108*, 2311, doi:10.1029/2002JB002290, 2003.

Davis, J. L., P. Elósegui, J. X. Mitrovica, and M. E. Tamisiea, Climate-driven deformation of the solid earth from GRACE and GPS, *Geophys. Res. Lett.*, *31*, L24605, doi:10.1029/2004GL021435, 2004.

Elósegui, P., et al., Climate-driven global three-dimensional deformation from GRACE, in preparation, 2004.

Farrell, W. E., Deformation of the Earth by surface loads, *Rev. Geophys.*, *10*, 761–797, 1972.

Flechtner, F., *AOD1B Product Description Document*, GR-GFZ-AOD-0001, Rev. 1, 2003.

Jekeli, C., Alternative methods to smooth the Earth's gravity field, Rep. 327, Dept. of Geod. Sci. and Surv., Ohio State Univ., Columbus, 1981.

Tamisiea, M., et al., Contribution of Alaskan glacier melting to global sea level change, in preparation, 2004.

Tapley, B., S. Bettadpur, J. C. Ries, P. F. Thompson, M. W. Watkins, GRACE measurements of mass variability in the Earth system, *Science*, *305*, 503–505, 2004.

Wahr, J. M., and J. L. Davis, Geodetic constraints on glacial isostatic adjustment, in *Ice Sheets, Sea Level, and the Dynamic Earth*, edited by J. X. Mitrovica and L. L. A. Vermeerson, Geodyn. Ser. 29, American Geophysical Union, 3–32, doi:10.1029/029GD02, 2002.

Wahr, J., S. Swenson, V. Zlotnicki, and I. Vellicogna, Time-variable gravity from GRACE: First results, *Geophys. Res. Lett.*, *31*, doi: 10.1029/2004GL019779, L11501, 2004.

Wahr, J., M. Molenaar, and F. Bryan, Time variability of the Earth's gravity field: Hydrological and oceanic effects and their possible detection using GRACE, *J. Geophys. Res.*, *103*, 30,205–30,230, 1998.

Wessel, P., and W. H. F. Smith, New version of the Generic Mapping Tools released, *Eos Trans. AGU*, *76*, 329, 1995.

Figure Captions

Fig. 1. Example time series for GRACE Stokes coefficients (shown as $\pm 1\sigma$ error bars) and best-fit to Eq. (6) (gray line).

Fig. 2. Top: Degree amplitudes for the GRACE errors. The blue line are the observed degree amplitudes, the dotted red line are the GRACE baseline values, and solid red line is the GRACE baseline scaled by 47. Middle: Degree amplitudes for the errors in the annual amplitudes (red) compared to the degree amplitudes for the estimated parameters (blue). Bottom: Degree amplitudes for the errors in the rate (red) compared to the degree amplitudes for the estimated parameters (blue).

Fig. 3. Observed in-phase (top) and out-of-phase (bottom) annual radial deformation amplitudes, reconstructed using the observed annual amplitudes and Eq. (9).

Fig. 4. Larger-scale figure focusing on annual amplitudes for South America. The top row is calculated using the F-test filtering of Eq. (9). The middle row is calculated using Gaussian smoothing with a radius at half-maximum of 1000 km, and the bottom row used a radius of 300 km . The left column is in-phase, and the right column is out-of-phase. Also shown are the locations of the GPS sites used in the comparison. The color scale is the same as that of Fig. 3.

Fig. 5. Comparison of GPS- and GRACE-determined annual amplitudes using the F-test filter (top) and Gaussian smoothing with radius 1000 km (middle) and 300 km (bottom). The GRACE amplitudes have been corrected for the absence of the $\ell = 1$ term in the GRACE data as described in Davis et al. (2004), which also describes the analysis of the GPS data.

Fig. 6. Weighted rms (wrms) fit for GPS-GRACE comparison for a range of smoothing radii. The filtered amplitudes yielded a wrms fit of 1.48 mm

Fig. 7. Observed geoid rates using Gaussian smoothing with 1000 km radius.

Figures

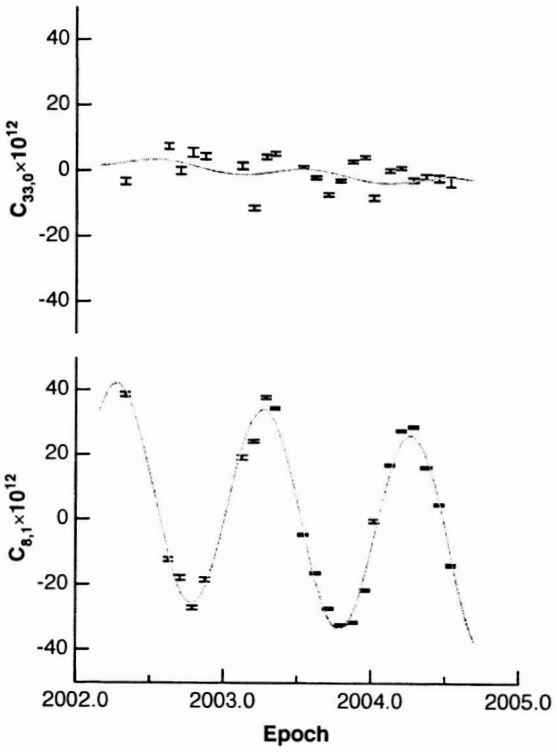

Fig. 1. Example time series for GRACE Stokes coefficients (shown as $\pm 1\sigma$ error bars) and best-fit to Eq. (6) (gray line).

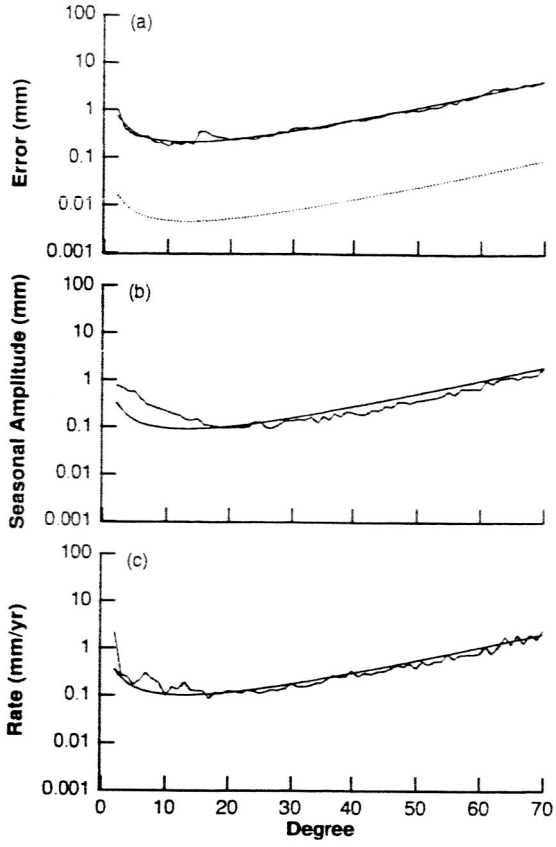

Fig. 2. Top: Degree amplitudes for the GRACE errors. The blue line are the observed degree amplitudes, the dotted red line are the GRACE baseline values, and solid red line is the GRACE baseline scaled by 47. Middle: Degree amplitudes for the errors in the annual amplitudes (red) compared to the degree amplitudes for the estimated parameters (blue). Bottom: Degree amplitudes for the errors in the rate (red) compared to the degree amplitudes for the estimated parameters (blue).

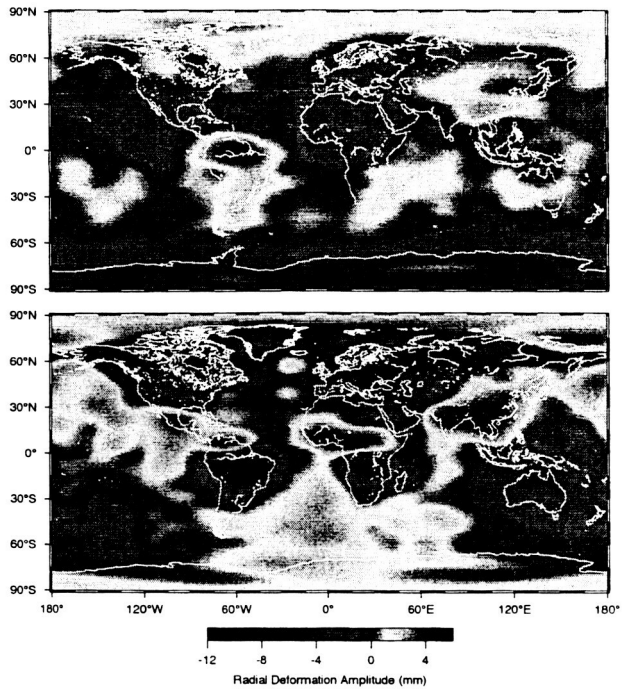

Fig. 3. Observed in-phase (top) and out-of-phase (bottom) annual radial deformation amplitudes, reconstructed using the observed annual amplitudes and Eq. (9).

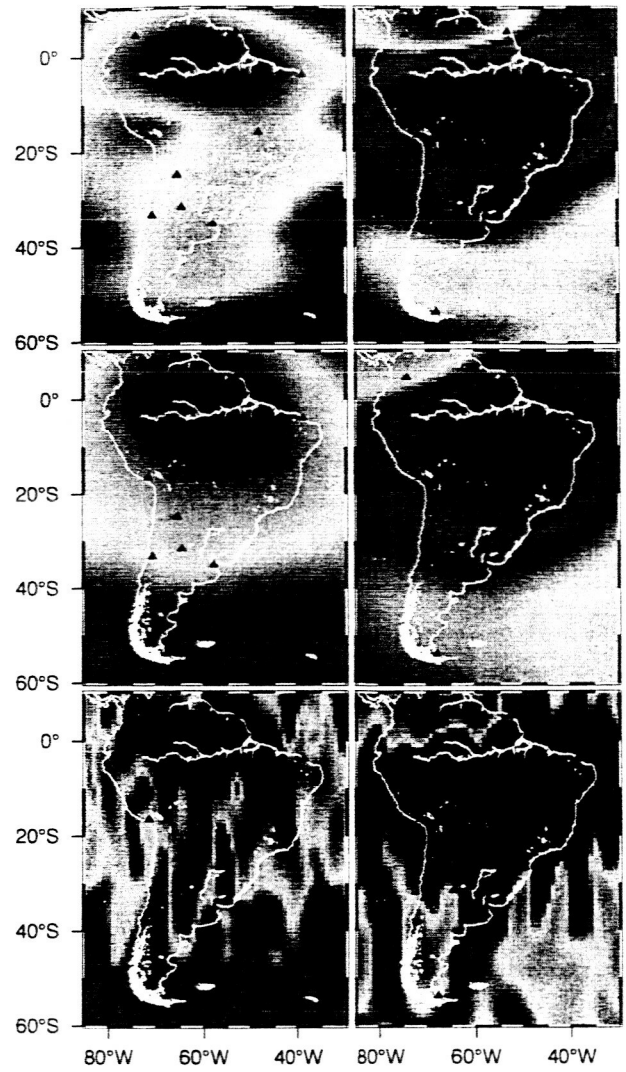

Fig. 4. Larger-scale figure focusing on annual amplitudes for South America. The top row is calculated using the F-test filtering of Eq. (9). The middle row is calculated using Gaussian smoothing with a radius at half-maximum of 1000 km, and the bottom row used a radius of 300 km . The left column is in-phase, and the right column is out-of-phase. Also shown are the locations of the GPS sites used in the comparison. The color scale is the same as that of Fig. 3.

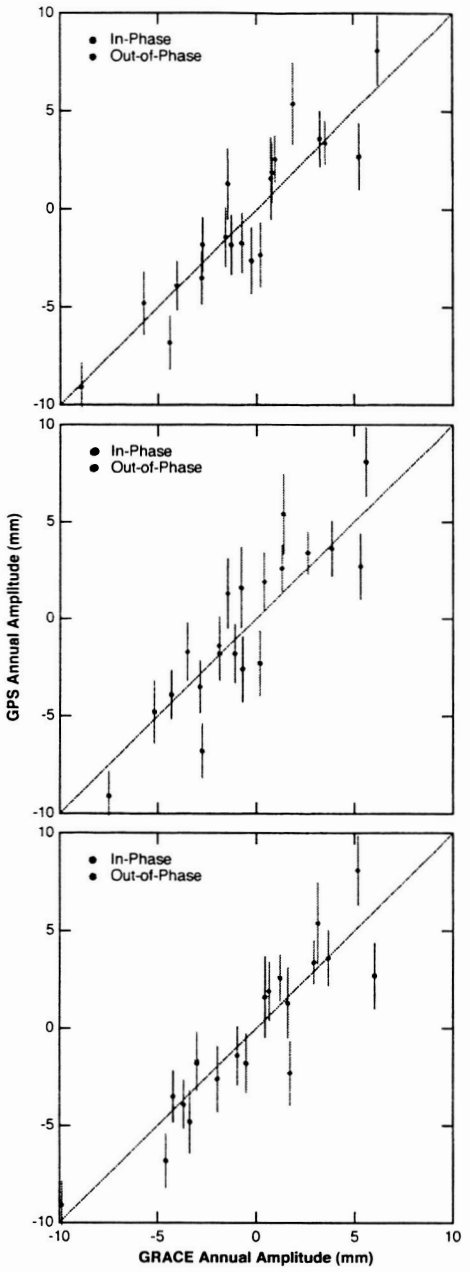

Fig. 5. Comparison of GPS- and GRACE-determined annual amplitudes using the F-test filter (top) and Gaussian smoothing with radius 1000 km (middle) and 300 km (bottom). The GRACE amplitudes have been corrected for the absence of the $\ell = 1$ term in the GRACE data as described in Davis et al. (2004), which also describes the analysis of the GPS data.

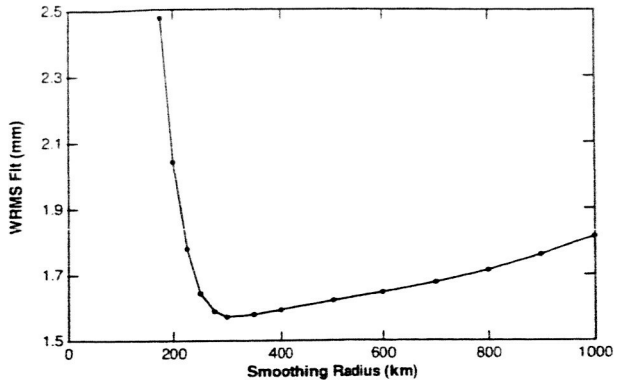

Fig. 6. Weighted rms (wrms) fit for GPS-GRACE comparison for a range of smoothing radii. The filtered amplitudes yielded a wrms fit of 1.48 mm

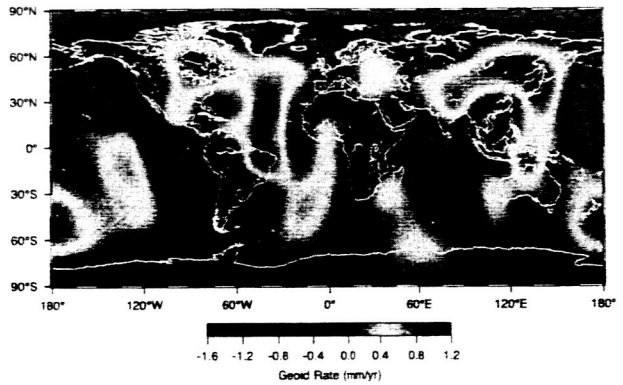

Fig. 7. Observed geoid rates using Gaussian smoothing with 1000 km radius.